Chinese Chemical Letters 35 (2024) 109352

Contents lists available at ScienceDirect

Chinese Chemical Letters

journal homepage: www.elsevier.com/locate/cclet

Tuning hot carrier transfer dynamics by perovskite surface modification

Chenghao Ge[a,1], Peng Wang[a,1], Pei Yuan[a,1], Tai Wu[a,1], Rongjun Zhao[b,*], Rong Huang[a], Lin Xie[a,*], Yong Hua[a,*]

[a] School of Materials and Energy, Yunnan University, Kunming 650091, China
[b] Department of Physics, Center for Optoelectronics Engineering Research, Yunnan University, Kunming 650091, China

ARTICLE INFO

Article history:
Received 25 October 2023
Revised 15 November 2023
Accepted 27 November 2023
Available online 2 December 2023

Keywords:
Perovskite solar cells
Interface passivation
Hot carrier
Charge recombination
Stability
Naphthalimide

ABSTRACT

Understanding the role of perovskite surface passivators in hot carriers transfer dynamics is important to develop highly efficient perovskite solar cells (PSCs). In this work, we have designed and synthesized a naphthalimide-based organic small molecule (NCN) for perovskite surface defect passivator. We reveal that the introduction of NCN not only reduces the density of perovskite defect-state, but also promotes hot carriers (HCs) cooling in perovskite through the transient absorption spectroscopy measurements. Fast HCs cooling permits HCs transfer from perovskite layer into NCN layer, thus resulting in the decreased charge-carrier recombination in NCN-treated device. As expected, the power conversion efficiency (PCE) of PSCs with NCN is enhanced to 22.02% from 19.95% for the control device. The findings are relevant for developing highly efficient PSCs.

Organic-inorganic perovskite solar cells (PSCs) have attracted the attention of large number of researchers due to their advantages such as high carrier mobility, adjustable band gap, long carrier diffusion length and large absorption coefficient [1–3]. Currently, the power conversion efficiency (PCE) of PSCs has exceeded 26% [4], which can even be comparable to silicon solar cells. Although their excellent PCEs, however, low operational stability is still a major obstacle for PSCs commercial application, which shows great rationality with these defects of perovskite layer. Since the crystalline growth process of perovskite materials at an uncontrollable condition, it is inevitable to produce some defects at the surface and grain boundary of the halide perovskite layer. It has been widely confirmed that these ionic defects tend to migrate and induce some holes in perovskite layer, which can facilitate the absorption of water molecules upon air exposure and the degradation of perovskite materials [5–8]. Moreover, these defects are usually regarded as non-radiative recombination centers, resulting in the severe deficit of charge extraction and transport by the charge transporting materials, which ultimately decreases the efficiencies of devices [9–12].

In order to solve these above-mentioned problems induced by perovskite defects, researchers have proposed various strategies, including perovskite crystallization control, perovskite composition optimization, surface and additive engineering, and charge carrier transport layer development [13–20]. Among them, the perovskite top surface modification between the perovskite-based light absorber layer and hole transport layer (HTL) has been the most straightforward and effective strategy for efficient and stable PSCs, which not only can effectively reduce the surface defects of the perovskite films, but also improve the contact at perovskite/HTL interface as well as promote the energy level matching between the perovskite active layer and HTL [21–24]. Therefore, it is meaningful to develop novel functional materials for passivating perovskite defect in highly efficient and stable PSCs. Although the rapid development in perovskite solar cells strongly promoted by passivating defects, the influence of passivation materials on the hot carriers (HC) transfer dynamics in perovskite absorber is still less explored. In this work, we have designed and synthesized a naphthalimide-based organic small molecule as perovskite surface passivation material (NCN), as shown in Fig 1a. It was found that NCN can strongly anchor on the top surface of perovskite layer by the chemical interaction between the carbonyl (C=O) and the uncoordinated lead ion in perovskite films, thus effectively passivating these surface defects as well as enhancing PSCs efficiency and long-term stability.

* Corresponding authors.
E-mail addresses: rjzhao@mail.ynu.edu.cn (R. Zhao), l.xie@ynu.edu.cn (L. Xie), huayong@ynu.edu.cn (Y. Hua).
[1] These authors contributed equally to this work.

https://doi.org/10.1016/j.cclet.2023.109352
1001-8417/

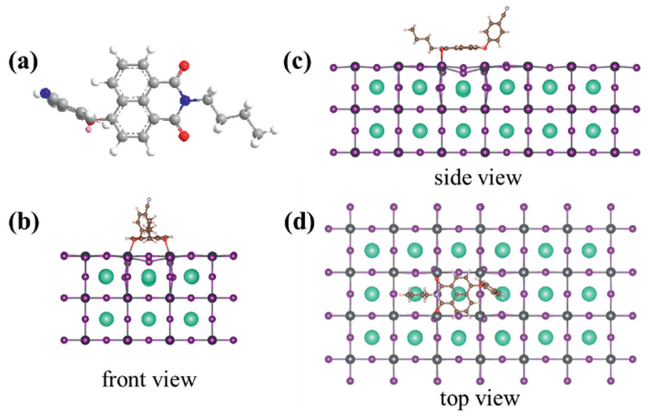

Fig. 1. (a) Molecular chemical structure of NCN. (b-d) Equilibrated structure (front view, side view, top view) of the perovskite surface passivated with NCN.

As shown in Scheme S1 (Supporting information), the targeted compound NCN was prepared according to two simple procedures, and the experimental details are provided in the supporting information. NCN was determined with the proton nuclear magnetic resonance spectroscopy and mass spectrometry, and the analysis results are shown in Figs. S1 and S2 (Supporting information). First, density functional theory (DFT) calculations were performed to gain insight into the interaction between NCN and perovskite. As shown in Figs. 1b-d, the geometry-optimized structures illustrate that the two oxygen atoms of NCN molecules can bind with the Pb atoms at the surface of perovskite material.

X-ray photoelectron spectroscopy (XPS) was used to study the interaction between perovskite and NCN. As shown in Fig. 2a, the O 1s spectrum of the perovskite/NCN films shows an obvious signal of Pb-O compared with the control perovskite films. Additionally, the Pb 4f peaks in perovskite/NCN sample move to lower binding energy with comparison to the control one (Fig. S3 in Supporting information). The XPS results suggest the interaction existence of NCN molecules and perovskite, which helps passivating trap states of perovskite films [25]. We further investigate the interaction by Fourier-transform infrared spectroscopy (FTIR) (Fig. S4 in Supporting information). The peak at 1698 cm^{-1} is the stretching vibration of the C=O group of NCN, which is shifted to 1694 cm^{-1} in NCN/PbI_2 sample, confirming the interaction between NCN and perovskite. Fig. 2b shows X-ray diffraction of perovskite films without and with NCN. Clearly, the intensity of PbI_2 characteristic peak at 12.7° in perovskite films with NCN is weaker than that of the control films, confirming that NCN can strongly passivate the perovskite defects. To quantitatively study the defect density, electron-only devices without and with NCN was fabricated to measure the trap density of perovskite films employing the space charge limited current (SCLC) method. As shown in Fig. S5 (Supporting information), the trap-filled limited voltage (V_{TFL}) of NCN treated device is decreased to 0.18 V from 0.42 V for the control device. Thus, the perovskite films treated with NCN delivers a lower trap state density (N_t) value of 2.37×10^{15} cm^{-3} than that of the control films (5.53×10^{15} cm^{-3}), which confirms the reduced perovskite defect density after NCN treatment.

We then fabricated PSCs with an architecture of FTO/SnO_2/perovskite/Spiro-OMeTAD/Ag to evaluate the effect of NCN on device photovoltaic performance. The photocurrent density *versus* voltage (*J–V*) curves of the control and NCN-treated devices are presented in Fig. 2c. The control device yields a PCE of 19.95% with a short-circuit current density (J_{SC}) of 24.63 mA/cm^2, an open-circuit voltage (V_{OC}) of 1.09 V, and a fill factor (FF) of 0.746. These photovoltaic parameters are enhanced with the introduction of NCN, the device exhibits a PCE of 22.02%, with a J_{SC} of 24.85 mA/cm^2, a V_{OC} of 1.14 V, and an FF of 0.776. Meanwhile, the device treated with NCN exhibits reduced hysteresis. The statistical PCEs of 40 devices are shown in Fig. S6 (Supporting information). The results reveal that the NCN-treated devices exhibit a higher average PCE with better reproducibility than that of the control devices. Moreover, the NCN-based device exhibits a higher stabilized PCE output of 21.86% with relative to the control one (19.21%) (Fig. S7 in Supporting information). Then, we further evaluated the long-term stability of these devices stored under nitrogen. As displayed in Fig. S8 (Supporting information), the NCN-based device exhibits better stability with retaining 94% of its initial efficiency after 800 h, while the control device only remains 74% of the original value. The enhanced stability of NCN-based device could be ascribed to the high hydrophobicity of perovskite surface after NCN treatment (Fig. S9 in Supporting information).

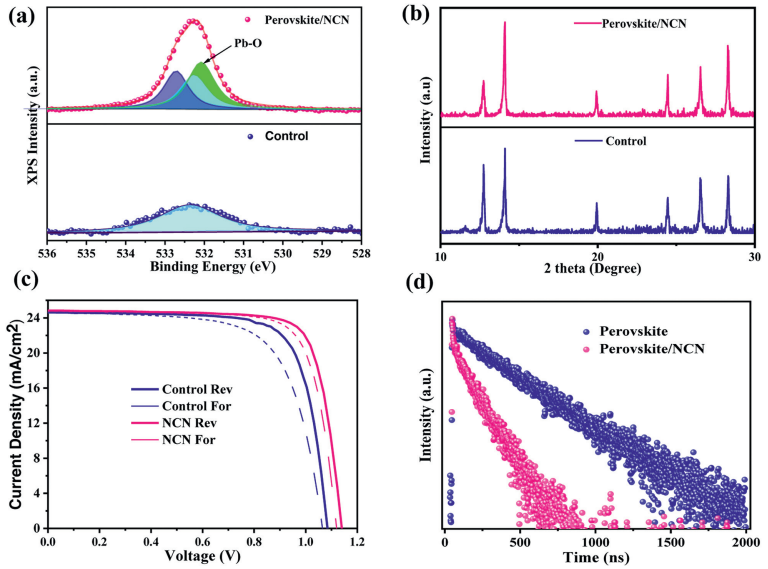

Fig. 2. (a) O 1s of XPS spectra of perovskite films without and with NCN. (b) XRD patterns of the control and perovskite films with NCN. (c) *J–V* curves of the control and NCN-based devices. (d) TRPL spectra of perovskite films without and with NCN.

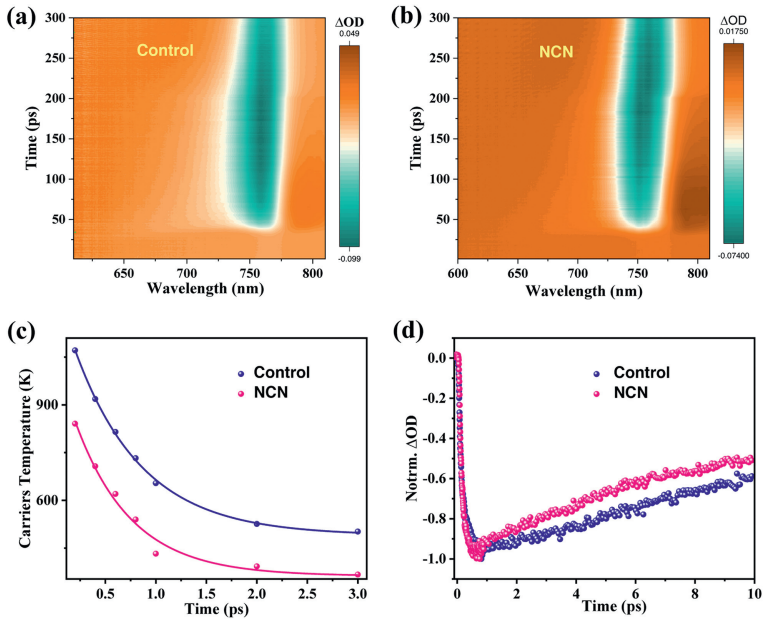

Fig. 3. (a, b) 2D pseudo-color plots of fs-TA spectrum of perovskite films pumped at 475 nm. (c) Extracted hot carriers temperature with delay time. (d) Normalized bleaching dynamics of perovskite films.

AFM was employed to investigate the effect of NCN on the top surface of perovskite layer. As shown in Fig. S10 (Supporting information), the root-mean-square (RMS) roughness of perovskite films is decreased from 21.5 nm to 18.7 nm upon NCN treatment, indicating a smoother film in NCN-treated perovskite sample, which would be favourable for enhancing the interfacial contact and charge transfer between perovskite layer and HTL. To gain insight into the improved performance in NCN-treated device, steady-state photoluminescence (PL) and time-resolved photoluminescence (TRPL) measurements were performed. As shown in Fig. S11 (Supporting information), a decreased PL intensity is observed for the FTO/SnO_2/perovskite/NCN sample compared with the control perovskite films with NCN, indicating better charge carriers (electron) transport from NCN-treated perovskite films into SnO_2-based ETL. Fig. 2d shows TRPL spectra of these samples, and their fitted data is listed in Table S1 (Supporting information). The control sample exhibits an average decay lifetime of 373.1 ns, whereas the target sample shows a shorter decay lifetime of 126.7 ns. The results further confirm that the electron transfer in NCN-treated sample is more efficient.

In order to fully understand the transfer dynamics of photoexcited hot carriers in device, which can be accessible by femtosecond transient absorption spectroscopy (fs-TA). Figs. 3a and b display the 2D *pseudo*-color TA plots of these two samples probed at 475 nm. Upon photoexcitation, a strong photobleaching (PB) band at around 760 nm is observed in both samples owing to the band-filling effect [26–28]. Figs. S12 and S13 (Supporting information) compare the normalized the time-dependent TA spectra from 0.2 ps to 3.0 ps. The broad high-energy tails (black arrow) near the PB band observed in TA spectra represent the hot carriers cooling process [26]. We found that the tail of perovskite/NCN films becomes narrower with continuously increasing the time compared with the pristine perovskite films, indicating the existence of NCN accelerates the hot carriers cooling that is usually assessed with the average carrier temperature (T_C) [29–32]. Fig. 3c displays the time dependence of T_C for these samples. Clearly, both films show continue T_C drop with the decay time, meanwhile, the perovskite/NCN sample shows much lower initial T_C value than that of the control one, which confirms a fast hot carriers cooling in NCN-treated perovskite films. Fig. 3d shows the kinetic profiles of perovskite films without and with NCN, and the fitted parameters are listed in Table S2 (Supporting information). The average hot carriers lifetime (τ_{avg}) decreases from 4.73 ps for the pristine perovskite films to 3.49 ps for perovskite/NCN films, further confirming that photogenerated hot carriers of perovskite layer can be extracted by the NCN layer, which is good for transporting the charge carriers and suppressing the charge recombination in device, consequently improving device performance. Fig. S14 (Supporting information) displays the kinetic decay lifetime of perovskite/Spiro-OMeTAD films without and with NCN. The τ_{avg} value of the control perovskite/Spiro-OMeTAD sample is 2.70 ps, which is reduced to 2.07 ps for perovskite/NCN/Spiro-OMeTAD sample, confirming the improved hot hole transfer from perovskite layer to HTL after NCN treatment.

To better understand the charge recombination process, light intensity (P_{light})-dependent J_{SC} characterizations were measured for these devices, which are fitted by the equations of $J_{SC} \propto P_{light}^{\alpha}$ [24,25]. As shown in Fig. 4a, NCN-treated device obtains a larger slope value ($\alpha = 0.997$) than that of the control device ($\alpha = 0.986$), indicative of a reduced interfacial charge carrier recombination in NCN-based device [33,34]. Then, we further used transient photovoltage (TPV) decay to investigate quantitatively the charge carrier lifetime in these devices. Fig. 4b reveals that the device with NCN treatment achieves a longer decay lifetime of 325 μs than that of the control device (189 μs), clearly demonstrating the decreased charge carrier recombination by the NCN modification [35], finally in turn contributing to the enhanced V_{OC} in PSCs.

In this work, we have designed and synthesized a naphthalimide-based organic small molecule (NCN) as an effective perovskite interface modifier. The NCN treatment can effectively reduce the trap-state density of the perovskite interface owing to the interaction between NCN and perovskite. The fs-TA observation found that the photogenerated hot carriers can be efficiently transported from perovskite layer to NCN molecules, and thus strongly suppressing the charge carrier recombination in device. Finally, the PCE of PSCs with NCN is enhanced to 22.02% from 19.95% for the control device. These results provide some insights for designing new passivating materials and understanding

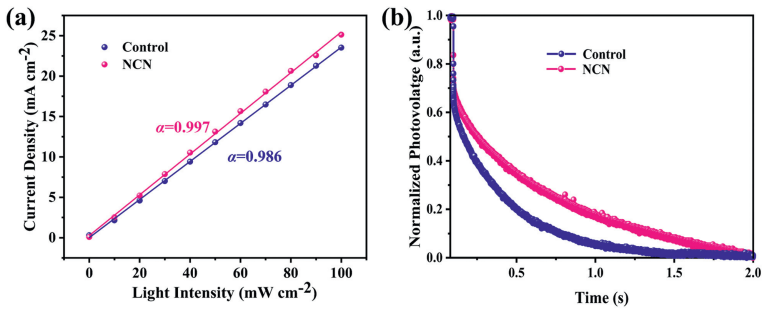

Fig. 4. (a) J_{SC} *versus* light intensity of devices. (b) The transient photovoltage (TPV) decay curves of PSCs.

hot carriers transfer in perovskites that is very important factor for enhancing PSCs performance.

Declaration of competing interest

The authors declare that they have no known competing financial interests or personal relationships that could have appeared to influence the work reported in this paper.

Acknowledgments

Y. Hua thanks High-Level Talents Introduction in Yunnan Province (No. C619300A010), the Fund for Excellent Young Scholars of Yunnan (No. 202001AW070008), Spring City Plan: the High-level Talent Promotion and Training Project of Kunming (No. 2022SCP005) for financial support. R. J. Zhao acknowledges the support from the Postdoctoral Foundation of Department of Human Resources and Social Security of Yunnan Province (No. C615300504046) and Postdoctoral Research Foundation of Yunnan University (No. W8223004). L. Xie thanks the National Natural Science Foundation of China (No. 22209144), the Project of Natural Science Foundation of Yunnan (Nos. 202101AU070034 and 202101AT070337). R. Huang thanks the Innovation and Entrepreneurship Training Program for college students (No. 202110673032). The authors thank the Electron Microscopy Center, the Advanced Analysis and Measurement Center of Yunnan University for the sample testing and service.

Supplementary materials

Supplementary material associated with this article can be found, in the online version, at doi:10.1016/j.cclet.2023.109352.

References

[1] S. Bai, P. Da, C. Li, et al., Nature 571 (2019) 245–250.
[2] Q. Jiang, J. Tong, Y. Xian, et al., Nature 611 (2022) 278–283.
[3] Z. Li, B. Li, X. Wu, et al., Science 376 (2022) 416–420.
[4] Best Research Cell Efficiency Chart, https://www.nrel.gov/pv/cell-efficiency.html.
[5] J. Kim, S.H. Lee, J.H. Lee, et al., J. Phys. Chem. Lett. 5 (2014) 1312–1317.
[6] S. Akin, N. Arora, S.M. Zakeeruddin, et al., Adv. Energy Mater. 10 (2020) 1903090.
[7] W. Xiang, Z. Wang, D.J. Kubicki, et al., Joule 3 (2019) 205–214.
[8] B. Cheng, T.Y. Li, P.C. Wei, et al., Nat. Commun. 9 (2018) 5196.
[9] J.J. Chen, N.G. Park, ACS Energy Lett. 5 (2020) 2742–2786.
[10] J.Z. Ye, M.M. Byranvand, C.O. Martnez, et al., Angew. Chem. Int. Ed. 60 (2021) 21804–21828.
[11] J.M. Ball, A. Petrozza, Nat. Energy 1 (2016) 16149.
[12] J.M. Xia, C. Liang, H. Gu, et al., Energy Environ. Mater. 6 (2023) e1196.
[13] M. Saliba, T. Matsui, K. Domanski, et al., Science 354 (2016) 206–209.
[14] M. Abdi-Jalebi, Z. Andaji-Garmaroudi, S. Cacovich, et al., Nature 555 (2018) 497–501.
[15] R.X. Lin, J. Xu, M.Y. Wei, et al., Nature 603 (2022) 73–78.
[16] N.X. Li, S.X. Tao, Y.H. Chen, et al., Nat. Energy 4 (2019) 408–415.
[17] R.M. Zhao, L. Xie, R.S. Zhuang, et al., ACS Energy Lett. 6 (2021) 4209–4219.
[18] T.Q. Niu, W.Y. Zhu, Y.H. Zhang, et al., Joule 5 (2021) 249–269.
[19] Y. Shao, Z. Xiao, C. Bi, Y. Yuan, J. Huang, Nat. Commun. 5 (2014) 5784.
[20] Y.N. Sun, W. Chen, Z.Y. Sun, Chin. Chem. Lett. 33 (2022) 1772.
[21] P.L. Qin, G. Yang, Z.W. Ren, et al., Adv. Mater. 30 (2018) e1706126.
[22] C.M. Wolff, P. Caprioglio, M. Stolterfoht, et al., Adv. Mater. 31 (2019) 1902762.
[23] Y. Shao, Y. Yuan, J. Huang, Nat. Energy 1 (2016) 15001.
[24] C. Chen, C. Wu, X. Ding, et al., Nano Energy 71 (2020) 104604.
[25] T. Wu, R.j. Zhao, D.L. Jia, et al., J. Energy Chem. 77 (2023) 517–520.
[26] J.H. Fu, S. Ramesh, J.W.M. Lim, Chem. Rev. 13 (2023) 8154.
[27] T. Zhu, Y. Wan, L.B. Huang, Acc. Chem. Res. 50 (2017) 1725–1733.
[28] P.P. Joshi, S.F. Maehrlein, X.Y. Zhu, Adv. Mater. 31 (2019) 1803054.
[29] T.C. Sum, N. Mathews, G.C. Xing, et al., Chem. Res. 49 (2016) 294–302.
[30] Q. Lai, R.S. Zhuang, K. Zhang, et al., Angew. Chem. Int. Ed. 62 (2023) e202305670.
[31] M. Li, J. Fu, Q. Xu, T.C. Sum, Adv. Mater. 31 (2019) 1802486.
[32] J.H. Fu, Q. Xu, G.F. Han, et al., Nat. Commun. 8 (2017) 1300.
[33] L. Yang, H. Zhou, Y.W. Duan, et al., Adv. Mater. 35 (2023) 2211545.
[34] S. Jiang, S.B. Xiong, W. Dong, et al., Adv. Sci. 9 (2022) 2203681.
[35] Y.T. Cheng, Q.B. Wei, N.N. Wang, et al., Chin. Chem. Lett. 34 (2023) 107933.